THE AMERICAN SOCIETY OF MECHANICAL ENGINEERS
345 E. 47th St., New York, N.Y. 10017

96-GT-100

TRANSITION EFFECTS ON SECONDARY FLOWS IN A TURBINE CASCADE

H. Moore and D.G.Gregory-Smith
School of Engineering,
University of Durham,
Durham, U.K.

BREAK

ABSTRACT

The regions of laminar and turbulent flow have been investigated in a linear cascade of a high turning HP rotor blades. Measurements of intermittency close to the blade and end wall surfaces have shown substantial areas of laminar and transitional flow. The implications for turbulence modelling are important, and Navier-Stokes computations have been performed to investigate how well transition can be modelled in such a flow. Using the intermittency data to specify transitional areas, the mixing length model of turbulence produces excellent results, although there is some sensitivity to the assumed freestream length scale. High Reynolds k-ε model results show too much turbulence and loss using the measured high inlet length scale, but the results are improved with the Kato-Launder modification. A low Reynolds number model does not seem to predict the transition effects, although more work is required with this model.

NOTATION

C_{ax}	Axial chord	u	Fluctuating component
C_p	(Uptream-Surface) pressure coeff.		
k	Turbulent kinetic energy	V_{ex}	Nominal exit velocity
L	Mixing length scale	y^+	Shear Reynolds number
S	Strain rate	ε	Turbulent k.e. dissipation rate
t	Time	Ω	Vorticity
$\bar{U}$	Mean velocity		Coefficients are made dimensionless by inlet velocity

INTRODUCTION

The design of turbomachinery components is becoming increasingly dependent on computational fluid dynamics (CFD) as computer hardware and software becomes more powerful. The validation of computer codes against experimental data is essential to give confidence in the results of CFD. The validation process requires the detailed study of the predictions through individual and sometimes idealised components as well as large scale comparisons of complete machine performance.

Experimental work at Durham University has studied the detail of the flow in a turbine cascade, in which there are large secondary flows, see Gregory-Smith & Cleak (1992). The flow is characterised by three main vortices. Around the leading edge, the inlet boundary layer gives rise to the horseshoe vortex, similar to that formed around a circular cylinder placed on an endwall. The legs of the horseshoe vortex are not symmetrical; the suction side leg runs close to the blade surface and then moves up the suction surface, while the pressure side leg crosses the passage and merges with the large passage vortex. The centre of the passage vortex starts close to the pressure surface on the end wall, moves towards the suction surface, and then migrates away from the end wall up the suction surface. The passage vortex sweeps up the upstream end wall boundary layer into a loss core, and a new highly skewed boundary layer is formed on the end wall. A much smaller counter vortex is formed in the corner between the end wall and the suction surface. These features also seen by other workers have been reviewed in detail by Sieverding (1985).

This data has been used as one of the test cases for a series of seminar/workshops organised by the European Research Community On Flow Turbulence And Combustion (ERCOFTAC), see Gregory-Smith (1993). A large number of different computations have been made by various workers of the secondary flow in this cascade, and some of them have been reviewed by Gregory-Smith (1995). It was shown that there is a wide variation between the codes in their predictions, part of the reason being the transitional nature of the flow and the consequent problems in turbulence and transitional modelling. Cleak et. al. (1991) showed that when using a

Presented at the International Gas Turbine and Aeroengine Congress & Exhibition
Birmingham, UK — June 10-13, 1996

mixing length model of turbulence, specifying the transition positions (from the experimental data) improved the predictions over those with fully turbulent flow.

Harrison (1989) measured the flow on the end wall of a similar cascade using hot film gauges. He showed that downstream of the separation line formed by the pressure side leg of the horseshoe vortex there are substantial regions of laminar flow. More recent work at Durham has concentrated on the secondary flows and turbulence close to the surfaces, see Moore & Gregory-Smith (1995), who found low values of turbulence close to the end wall except in the corner between the end wall and the suction surface. On the suction surface Halstead et. al. (1990) found that the boundary layer was laminar until shortly after the point of minimum surface pressure where a laminar separation bubble was formed with turbulent reattachment. Surface flow measurements in the Durham cascade by Walsh and Gregory-Smith (1987) indicated the same feature away from the end wall, but this was replaced by natural transition (or rather 'by-pass transition' as stated by Mayle, 1991) when an upstream grid produced high turbulence at cascade inlet, Gregory-Smith & Cleak (1992). One objective of this paper is to present quantitative data of the intermittency of the flows close to the end wall, suction and pressure surfaces, thereby giving information on the laminar, turbulent and transitional regions.

A second objective is to present the results of various turbulence models on the predictions of a well established turbomachinery CFD code developed by Rolls-Royce. The models used are mixing length and high and low Reynolds number k-ε models. The overall aim is to assess the importance of the transition process in the flow predictions, making use of the quantitative data provided by the intermittency measurements.

EXPERIMENTS

Durham Cascade

The cascade contains rotor blades of some 110° of turning, similar to those of a high pressure axial flow turbine. The cascade geometry is described by Gregory-Smith & Cleak (1992). The blading design details are given in Table 1.

Table 1: Cascade Design Data

Inlet Flow Angle	42.75°
Blade Exit Angle	-68.7°
Blade Axial Chord, Cax	181 mm
Blade Half-Span	200 mm
Reynolds Number (Cax & Vex)	4.0×10^5
Exit Mach Number	0.1

There is an upstream turbulence grid to give high inlet turbulence as indicated in Table 2. There are three slots one axial chord upstream of the cascade, used to determine the inlet flow conditions, as described by Moore & Gregory-Smith (1995). There are also 11 traverse slots, one upstream, seven within the cascade and three downstream. It may be noted that the flow is low speed with the Reynolds Number less (about half) than that for a typical HP rotor blade. This means that the flow may be a little more dominated by transition, and so it may be a rather more exacting CFD test case than an actual blade might be.

Table 2: Inlet Flow, One Axial Chord Upstream

Free Stream:	
Inlet Angle	43.5°
Streamwise Turbulence Intensity	5.1%
Spanwise Turbulence Intensity	5.6%
Normal Turbulence Intensity	5.0%
Turbulent k.e. Coefficient	0.0083
Turbulent Dissipation Rate	32.6 m^2/s^3
Mixing Length Scale	9.4mm

Instrumentation

Measurements were made of the intermittency close to the end wall and blade pressure and suction surfaces. A single hot wire was mounted in a traverse gear through one of the traverse slots. A surface locating pin ensured the wire was at 1mm from the blade surface or endwall. A high speed A/D converter was used to log the signal at 50kHz with 8192 samples being taken at a time. This number was limited by the PC memory but testing showed that it was sufficient to give repeatable results.

The principle of intermittency measurement is straight forward. The signal from the anemometer is sampled for a period of time and the portion for which the flow is turbulent, characterised by large signal fluctuations, is calculated. In practice it can be difficult to distinguish between laminar and turbulent portions of the raw signal, and some processing is required. The technique used here was based on the Turbulent Energy Recognition Algorithm (TERA) method of Falco & Gendrich (1990), which has been found to work well even in regions of adverse pressure gradient and high freestream turbulence, see Walker & Solomon (1992). The function $\left| u \frac{du}{dt} / \bar{U} \right|$ was calculated, where $\bar{U}$ is the mean velocity and u the fluctuating component. A rolling average over 20 samples (400μs) was then used to smooth the data and a threshold was chosen, above which the flow is taken to be turbulent. The choice of threshold values was made by inspection of the traces, and although this is not ideal, attempts to devise a more formal method were not successful. Thus there is a certain margin of error in these results, but since the same criteria were used to choose the thresholds, the results should be reasonably self consistent. By taking several measurements at a given point and by investigating the effect of varying the threshold, an estimate was made of ±0.1 for the error in intermittency value. Full details of the instrumentation and the experimental technique are given by Moore (1995).

Experimental Results

Traverses at 1mm from the endwall were made at slot 1 upstream of the blades, slots 2-8 within the blade passage, and slots 9 & 10 downstream. The values of intermittency are shown in Figure 1 as a contour plot over the endwall. At the inlet, the intermittency is high (>0.8) with a dip towards the centre of the passage away from the horseshoe vortex legs. Close to the suction surface after the leading edge, the intermittency falls to 0.5 in the accelerating flow, indicating incipient relaminarisation. However this is terminated by the high intermittency (>0.9) associated with the separation line of the pressure side of the horseshoe vortex, as it crosses the blade passage from the adjacent blade. Behind the separation line there is a rapid reduction in intermittency, giving low values over much of the end wall where the new end wall boundary layer is formed. Thus it appears that a substantial region of the endwall flow is largely laminar. However near to the suction surface the intermittency remains very high in the region of the counter vortex in the corner between the endwall and suction surface. On proceeding downstream, the intermittency slowly rises with the region of fully turbulent flow spreading over the endwall. The results of Figure 1 compare well with Harrison's (1989) and with the measurements of the turbulent kinetic energy at 1.5mm from the end wall made by Moore & Gregory-Smith (1995), mentioned above.

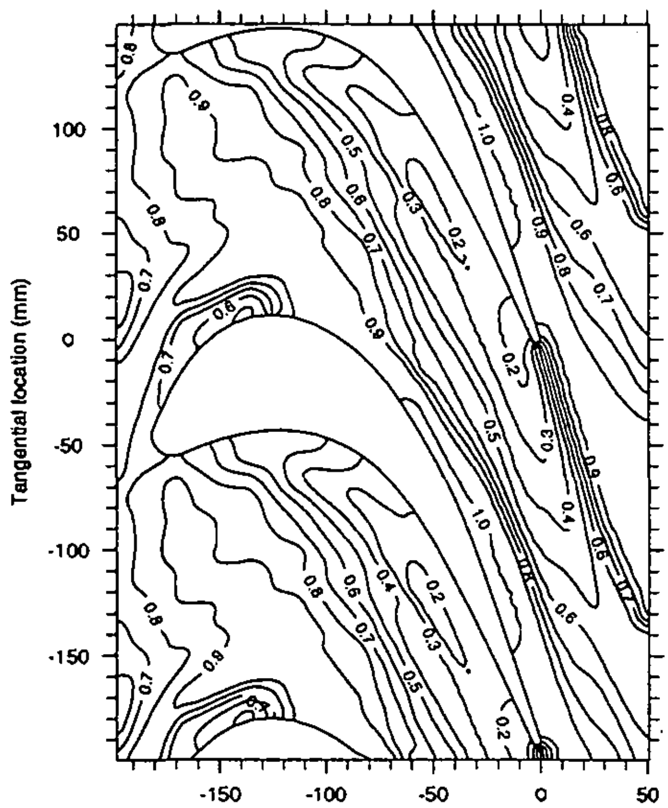

Figure 1: Intermittency 1.0mm. from the Endwall

On the suction surface of the blade, traverses were made from 1.5mm to 100mm from the endwall at slots 2-8 in the blade passage, from 6% to 97% Cax. The results are shown in the contour plot of Figure 2. Away from the endwall, the strong initial acceleration of the flow on the suction surface ensures a laminar boundary layer. Then from slot 6 onwards (71% Cax) the intermittency starts to rise indicating transition due to the slight diffusion of the flow towards the trailing edge. This agrees with earlier surface flow visualisation by Walsh and Gregory-Smith (1987) and Gregory-Smith & Cleak (1992), indicating transition at around 80% Cax at midspan Towards the endwall, there is a rapid rise in intermittency caused by the inlet endwall turbulent boundary layer, the horseshoe vortex and then the passage vortex. This region begins to spread as the passage vortex grows and moves away from the end wall. From slot 5 (55% Cax) the corner vortex and passage vortex produce two distinct ridges of high intermittency with a drop between them

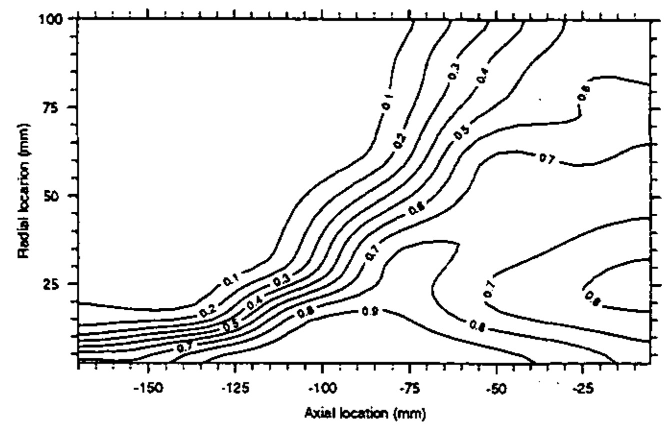

Figure 2: Intermittency 1.0mm from the Suction Surface

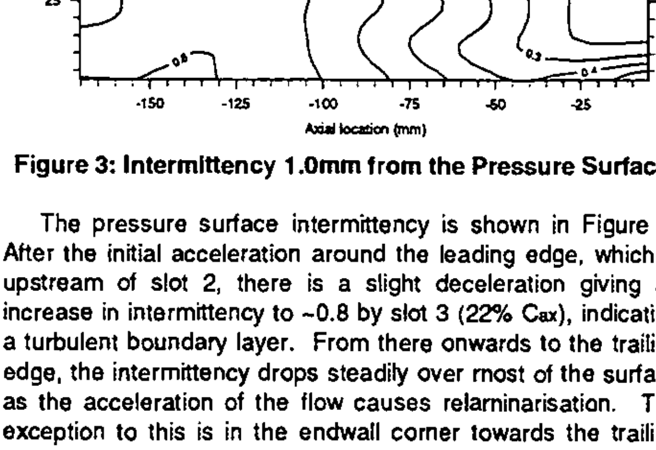

Figure 3: Intermittency 1.0mm from the Pressure Surface

The pressure surface intermittency is shown in Figure 3. After the initial acceleration around the leading edge, which is upstream of slot 2, there is a slight deceleration giving an increase in intermittency to ~0.8 by slot 3 (22% Cax), indicating a turbulent boundary layer. From there onwards to the trailing edge, the intermittency drops steadily over most of the surface as the acceleration of the flow causes relaminarisation. The exception to this is in the endwall corner towards the trailing edge. This is consistent with a corner vortex formed by the flow down the pressure surface towards the endwall. That it remains much smaller than the corner vortex in the suction corner is due to the strong acceleration of the flow along the pressure surface.

COMPUTATIONS

Numerical method.

The computational method used was a pressure correction method supplied by Rolls-Royce plc and based on the algorithm of Moore & Moore (1985). A particular feature of this method is the use of upwinded control volumes for the integration of the momentum equation thus allowing the use of central differencing to reduce numerical mixing, yet having a set of stable finite difference equations. In evaluating a computational method it is necessary to establish numerical grid independence so that the effects of different turbulence models can be distinguished. A comparison of various calculations of the Langston cascade (Lakshminarayana 1991) showed that the code of Moore & Moore gave better estimates of loss on a coarse grid compared with other methods. This implies that the Moore & Moore code is likely to give grid independence with a relatively coarse grid.

All calculations have been carried out on structured 'H' type grids. These were first created on the axial-tangential plane and used in two-dimensional calculations. They were then stacked in the spanwise direction to produce three-dimensional grids. Two grids were used, a coarse and fine grid. The coarse grid consists of 89 axial and 38 tangential points. Some grid points lie within the blade, allowing more orthogonal cells around the leading and trailing edges. The grid was designed to be used with wall functions with the near surface grid line lying within the log law region ($30 < y^+ < 100$). For the three-dimensional grid, it was stacked on 29 spanwise planes giving a total of 98078 points (89x38x29).

The fine grid consisted of 99 axial by 55 tangential points with a much finer near wall spacing of $y^+ < 3$ in order to resolve the flow into the laminar sublayer. This level of refinement inevitably leads to some highly skewed and high aspect ratio cells which are likely to give numerical problems. The three-dimensional grid had 42 spanwise planes giving a total grid size of 228690 points (99x55x42).

Turbulence Modelling.

Three turbulence models were used, a mixing length model, and high and low Reynolds number k-ε models. In addition a variant of the k-ε models called the S-Ω modification was used.

The mixing length model (due to Moore & Moore) was based on Prandtl's formulation for the length scale within a shear layer:

$$L = \min(\kappa y, \lambda\delta),$$

where $\kappa = 0.41$, $\lambda = 0.08$ and δ is the thickness of the shear layer. Outside the shear layer the effect of freestream turbulence is allowed for by varying L linearly to a specified freestream length scale at a slope no greater than κ. The turbulent viscosity is then set by:

$$\mu_T = \rho L^2 S F_{vd}^2,$$

where ρ is the density, S the strain rate and F_{vd} the Van Driest damping function.

The high Reynolds number k-ε model was essentially the Jones and Launder (1972) model where k and ε are the turbulent kinetic energy and its dissipation rate, obtained from the solution of convection-diffusion equations. From the logarithmic law of the wall, so called wall functions are used in the near wall cell.

The low Reynolds number k-ε model was that due to Launder and Sharma (1974). Such a model requires a very fine grid near a solid surface, thus requiring larger computer resources, but in principle it is capable of predicting transition.

One weakness of conventional k-ε models is that they may predict excessive levels of turbulence and hence turbulent viscosity, in regions of large irrotational strain. This is particularly important in irrotational flow near the leading edge stagnation point and in the strongly accelerating flow through the blade passage. The S-Ω modification of Kato and Launder (1993) can alleviate this problem by replacing S^2 in the production term for k by $S\times\Omega$, where Ω is the vorticity. Whilst this modification can be quite successful (see below) it should be noted it is not physically accurate as it introduces an inconsistency between the Reynolds stresses in the turbulence energy equation and the Reynolds-averaged Navier-Stokes equation (see Kato and Launder 1993).

TWO-DIMENSIONAL COMPUTATIONAL RESULTS

Mixing Length Model

Effect of Freestream Length Scale. With the mixing length model the freestream length scale is specified at inlet and does not vary through the flow, unlike the k-ε model where the convective equations allow its value to change. Using the inlet length scale from Table 2, the mixing length model produced much too much loss. Table 3 (for the coarse grid) shows that the effect of varying the inlet length scale are dramatic on the loss at the slot 10 (28% Cax downstream). They are compared with the experimental results obtained at mid-span by HM (Moore 1995), who made hot wire traverses and TB (Biesinger 1993), who traversed with a five-hole probe and so was able to obtain loss data. The highest length scale gives very high loss. The lowest length scale seems to give a result close to the experiment, but it should be remembered that the computation assumes turbulent flow everywhere and so the results should be above the experimental value.

Table 3: Effect of Freestream Length Scale at Slot 10

Length Scale	Yaw Angle	Loss Coeff.
9.4mm	-68.9	0.489
0.94mm	-69.0	0.171
0.094mm	-69.1	0.105
HM Experimental	-68.4	-
TB Experimental	-68.3	0.097

A further comparison is shown in Figure 4 which shows the variation of loss coefficient across the pitch at Slot 10. For the two smaller length scales the wakes are well defined, with the smallest value giving least wake spreading. The largest length scale gives an unrealistic wake spreading across the whole pitch. It appears therefore that the allowance for freestream turbulence in this mixing length model is not accurate for the largest length scale. Subsequent calculations with the mixing length model were done with L=0.94mm

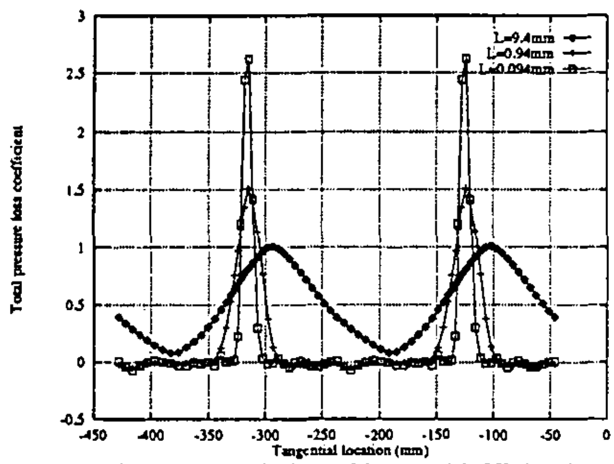

Figure 4: Pitchwise Variation of Loss with Mixing Length Model.

__Effect of Laminar Regions__ With the mixing length model, transition can be simulated by specifying the variation through the flow of a factor β which is a multiplier for the turbulent viscosity μ_T. The first three variations are summarised in Table 4 together with the resulting loss coefficient. As with the results above, the variation of yaw angle prediction was very slight and is omitted.

V1 was what Cleak et.al. (1991) had done at midspan for their 'laminar block A'. V2 makes upstream of the blades turbulent as it is in practice, and V3 gives a gradual instead of sudden transition. It can be seen that the effect of these specifications with substantial regions of laminar flow considerably reduces the loss coefficient compared to that in Table 3 for L=0.94mm. However neither the upstream flow specification or whether gradual or sudden transition is specified has much effect, a result that seems reasonable.

Table 4: Effect of β Variations 1-3 (L=0.94mm).

	Version	Axial Chord Range	Variation of β	Loss Coefficient
V1	Sudden Transition	$-1.0 \rightarrow 0.8$ $0.8 \rightarrow 1.0$	0 1	0.124
V2	Upstream Turbulent	$-1.0 \rightarrow 0.0$ $0.0 \rightarrow 0.8$ $0.8 \rightarrow 1.0$	1 0 1	0.125
V3	Gradual Transition	$-1.0 \rightarrow 0.6$ $0.6 \rightarrow 1.0$ $1.0 \rightarrow 2.0$	0 $0 \rightarrow 1.0$ 1	0.123

The above variations are based on the intermittency on the suction surface, whereas on the pressure surface it is quite different. Thus versions 4-6 allowed a pitchwise variation, as specified in Table 5. V4 gives mainly laminar flow in the mid-pitch until towards the trailing edge. V5 and V6 give the bulk of the fluid as turbulent except to within 10% or 5% of the surfaces. The resulting values of loss coefficient show that the difference in mainstream specification between V4 and V5 makes little difference, with values close to the experiment. However in V6 the flow is allowed to become turbulent too close to the blade surfaces as indicated by the rise in the loss.

The difference between V3 and V4 is effectively the specification of the pressure surface boundary layer. In V3 it is specified the same as the suction surface, i.e. becoming turbulent towards the trailing edge where the surface velocities are high. In V4 the correct relaminarisation towards the trailing edge is simulated giving laminar flow there and thus reducing the loss in the pressure surface boundary layer.

This study in 2D indicates the importance of laminar region specification and their effect in 3D may be expected to be significant also.

Table 5: β Variations 4-6, across Pitch.

Suction Surface		Pressure Surface	
Cax Range	Variation of β	Cax Range	Variation of β
$-1.0 \rightarrow 0.0$	1	$-1.0 \rightarrow 0.0$	1
$0.0 \rightarrow 0.05$	$1 \rightarrow 0$	$0.0 \rightarrow 0.8$	$1 \rightarrow 0$
$0.05 \rightarrow 0.6$	0	$0.8 \rightarrow 0.99$	0
$0.6 \rightarrow 0.99$	$0 \rightarrow 1.0$	$0.99 \rightarrow 1.0$	$0 \rightarrow 1.0$
$0.99 \rightarrow 2.0$	1	$1.0 \rightarrow 2.0$	1

	Extent of SS spec. (fraction pitch)	Between	Extent of PS spec.	Loss Coeff.
V4	$0.0 \rightarrow 0.9$	$0.9 \rightarrow 0.95$ ramp	$0.95 \rightarrow 1.0$	0.092
V5	$0.0 \rightarrow 0.1$ ramp	$0.1 \rightarrow 0.9$ β=1	$0.9 \rightarrow 1.0$ ramp	0.095
V6	$0.0 \rightarrow 0.05$ ramp	$0.05 \rightarrow 0.95$ β=1	$0.95 \rightarrow 1.0$ ramp	0.144

__k-ε Model of Turbulence.__

The results with the high Reynolds number k-ε model of turbulence can be seen in Table 6. The turbulent kinetic energy coefficient is also shown, giving an indication of the level of turbulence at slot 10. The standard model gives too much loss and turbulence and, as with the mixing length model using the measured inlet length scale, the loss was high across the whole pitch. The turbulent kinetic energy was also high across the pitch as can be seen in the upper blade of Figure 5. These results differ from the mid-span results of Cleak & Gregory-Smith (1992) who had low mid-pitch loss and turbulence. This is probably due to the lower assumed inlet length scale in those calculations (3.3mm) which meant that the effect of the excessive generation of turbulence in the standard model was much less. Their mid-span loss (with a much coarser grid) was 0.268. Here the S-Ω modification gives low loss and turbulence at mid-pitch, with well defined wakes and this can be seen in the lower blade of Figure 5. The averaged turbulence is rather high and the loss more so, but since the flow is assumed fully turbulent, this is to be expected.

Table 6: k-ε Model at Slot 10

Model	Length Scale	Loss Coeff.	k Coeff.
Standard	9.4mm	0.336	0.091
S-Ω mod.	9.4mm	0.208	0.014
Low Re. No.			
Standard	3.3mm	0.223	0.023
S-Ω mod.	3.3mm	0.214	0.008
HM Expt.		-	0.012
TB Expt.		0.097	-

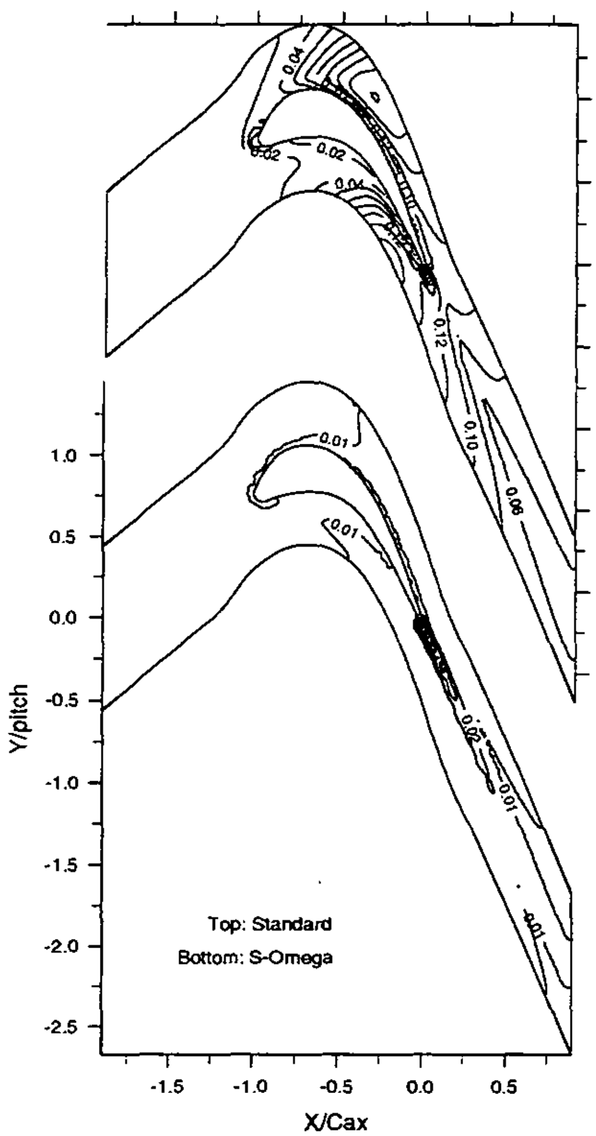

Figure 5: Turbulent K.E. Contours (2D Flow)

Some computations were also made with the low Reynolds number turbulence model with the fine grid. Some results were obtained with a reduced level of turbulence (4.5%) and length scale (3.3mm) at inlet and these are shown in Table 6 also. There is a reduction in loss compared to the standard high Reynolds number model, which is probably due largely to the lower inlet length scale, and the S-Ω model actually shows an increase. Thus there is little evidence here that the low Reynolds number is modelling the transition effects in a satisfactory manner.

THREE-DIMENSIONAL COMPUTATIONS

Mixing Length Model

Length Scale and Grid Refinement The effect of variation of inlet length scale and grid refinement is shown in Table 7 where data at slot 10 is given. The overall loss and midspan loss show the same effects as seen with the two-dimensional calculations, with reductions with smaller inlet length scale. The midspan here and two-dimensional results above are a little different due to end wall blockage. The secondary kinetic energy gives a measure of the strength of the passage vortex, and this is further seen in Figure 6. The large length scale gives low secondary velocities with little movement of the vortex centre, while the low length scale gives results close to the experiment. A comparison of the results from the coarse and fine grids shows little difference, indicating some degree of grid independency. The slight rise in loss with the fine grid in Table 7 is attributed to the poor grid quality near the surfaces. The mixed out values may be used to give the secondary loss. The low secondary flow with the high length scale gives a correspondingly low secondary loss, while the other two predictions are reasonable.

Table 7: 3D Mixing Length at Slot 10

Length Scale / Grid	9.4mm Coarse	0.94mm Coarse	0.94mm Fine	Experiment TB	Experiment HM
Loss	0.534	0.219	0.250	0.170	
Midspan Loss	0.482	0.148	0.185	0.097	
Sec. K.E.	0.005	0.027	0.026	0.017	0.016
Mixed Out Values					
Loss	0.544	0.274	0.279	0.189	
Midspan Loss	0.487	0.159	0.195	0.098	
Sec. Loss	0.053	0.115	0.084	0.091	

Further information is shown in Figure 7, where pitch averaged results at slot 10 are given. The yaw angle and loss are quite good for the low length scale, with the peak values reasonable and at the correct spanwise location. The poor performance with the high inlet length scale is very noticeable, with high loss and low under turning.

Effect of Laminar Regions As with the two-dimensional simulations, the effect of specifying the flow close to the endwall and pressure and suction surfaces was investigated. The flow at midspan was specified as in V5, and as the end wall was approached, the pattern indicated in Figure 2 was simulated. The flow on the end wall was simulated according to Figure 1. As in V5, the freestream was specified as turbulent, the freestream being defined as further than 10%

pitch from the blade surfaces and 15mm from the endwall. The area plots are shown in Figure 8, giving the total pressure loss contours, compared with the fully turbulent flow (with 0.94mm and coarse grid) from the previous section.

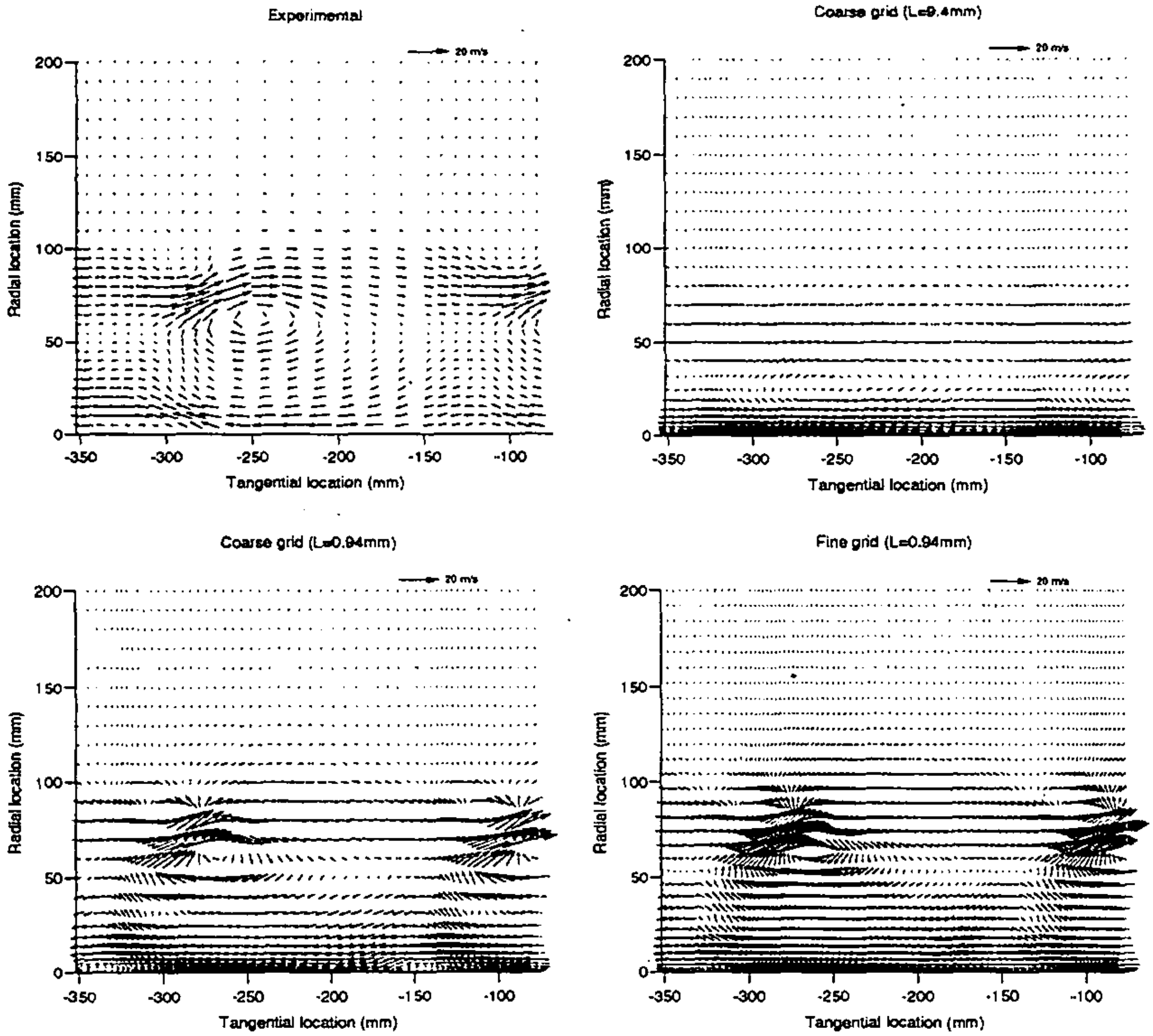

Figure 6: Secondary Flow at Slot 10 with Mixing Length Model

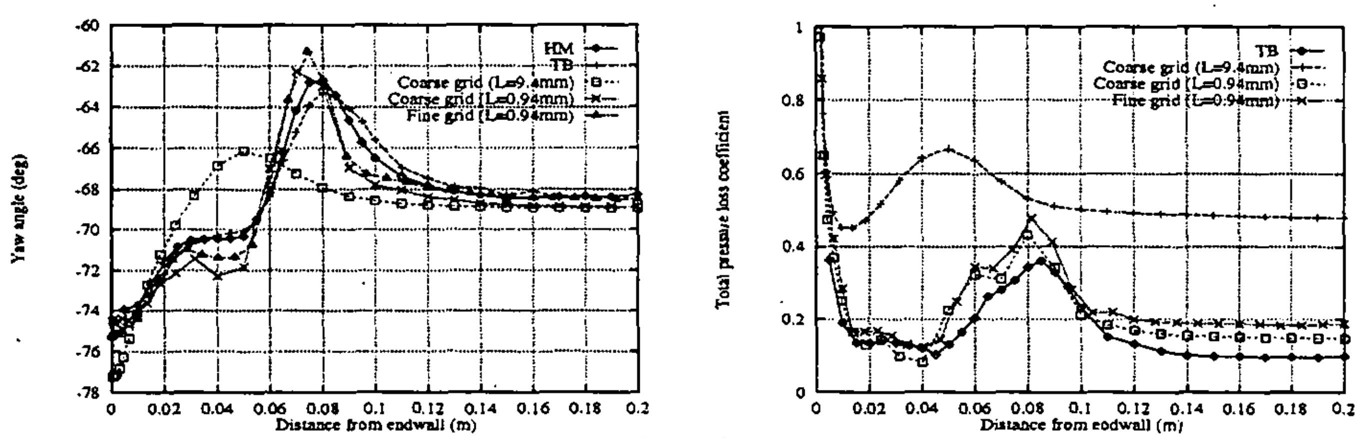

Figure 7: Pitch Averaged Results at Slot 10 with Mixing Length Model

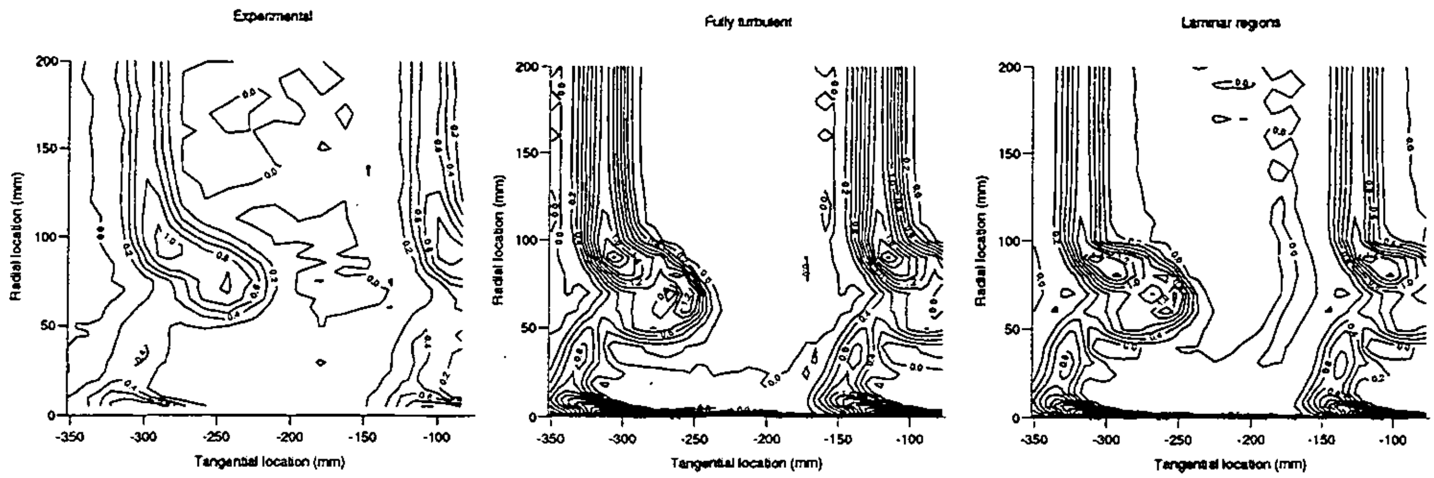

Figure 8 Total Pressure Loss Coefficient at Slot 10 with Mixing Length Model

The wake is noticeably less thick and the peak values in the loss core are reduced a little. The loss on the endwall is only slightly reduced with the laminar regions. The results from the TB experiment are also shown and are in close agreement with the computations, especially with the laminar regions. Quantitative information is given in Table 8. The effect of the laminar regions has been to reduce the losses, so that the experimental loss values are approached. The strength of the secondary velocities is slightly increased as the effect of the turbulent dissipation is reduced.

Table 8: Laminar Regions & k-ε Model at Slot 10

	Mixing Length		k-ε Model			Expt.
	Fully Turbulent	Laminar Regions	S^2	S-Ω	Low Re S-Ω	TB.
Loss	0.219	0.193	0.379	0.268	0.298	0.170
Midspan Loss	0.148	0.120	0.337	0.208	0.234	0.097
Sec. K.E.	0.027	0.028	0.009	0.018	0.017	0.017
Mixed Out Values						
Loss	0.274	0.231	0.394	0.288	0.328	0.189
Midspan Loss	0.159	0.126	0.344	0.218	0.244	0.098
Sec. Loss	0.115	0.105	0.050	0.070	0.078	0.091

k-ε Model of Turbulence

The secondary velocities for the high Reynolds number k-ε model are shown for both the standard (S^2) and S-Ω modification are shown in Figure 9, and may be compared to the experimental and mixing length results in Figure 6. The S^2 results show too low values and not enough vortex centre movement, However it is much better than the mixing length with the same inlet length scale, 9.4mm., showing the effect of the inlet length scale variation in the model. The S-Ω results are somewhat better, with more vortex movement, but not as much as with the lower inlet length scale for the mixing length model. Further information is given in Figure 10 where the pitch averaged yaw angle and loss are given, including the low Reynolds number model results. Again the S-Ω results are better, with the low and high Reynolds number models showing little difference. Table 8 also shows that the high Reynolds number model with the S-Ω modification gives better values than the standard version, although the losses are high and the secondary kinetic energy low. The low Reynolds number model gives even higher losses, indicating no satisfactory modelling of the transition.

GENERAL DISCUSSION

The intermittency measurements show that there are significant areas of laminar and transitional flow over the endwall and suction surface. While that on the suction surface is as expected, the endwall flow is very complex. There are laminar areas in the new endwall boundary layer behind the horseshoe vortex separation line, but with highly turbulent flow in the suction surface corner where the corner counter vortex is formed. This is in agreement with the findings of other investigators, but in addition the quantitative data provided here provides a valuable input into the CFD modelling process.

The mixing length model does not perform satisfactorily when a large free stream length scale is used. The value deduced from the k-ε model does fall, as expected, from the high value measured at inlet to about 50% within the passage. The tests with the mixing length model indicated a reduction to about 10% was necessary to get reasonable results.

When the intermittency data is used to specify regions of laminar and turbulent flow, the computational results using a simple mixing length model and low inlet length scale prove to be very satisfactory, both for two- and three-dimensional flow. Whether the freestream is defined as turbulent or not does not make very much difference to the results, but getting the relaminarisation effect on the pressure surface did give an improvement. The appearance of the secondary velocity vectors and loss contours at the downstream traverse slot agrees well with experiment, although the secondary kinetic energy (seen in Table 8) is above that measured. As Gregory-

Smith (1995) noted, an eddy viscosity model of turbulence is unlikely to generate the high values of turbulence seen in the loss core, and so too slow a decay of secondary kinetic energy downstream of the trailing edge is predicted

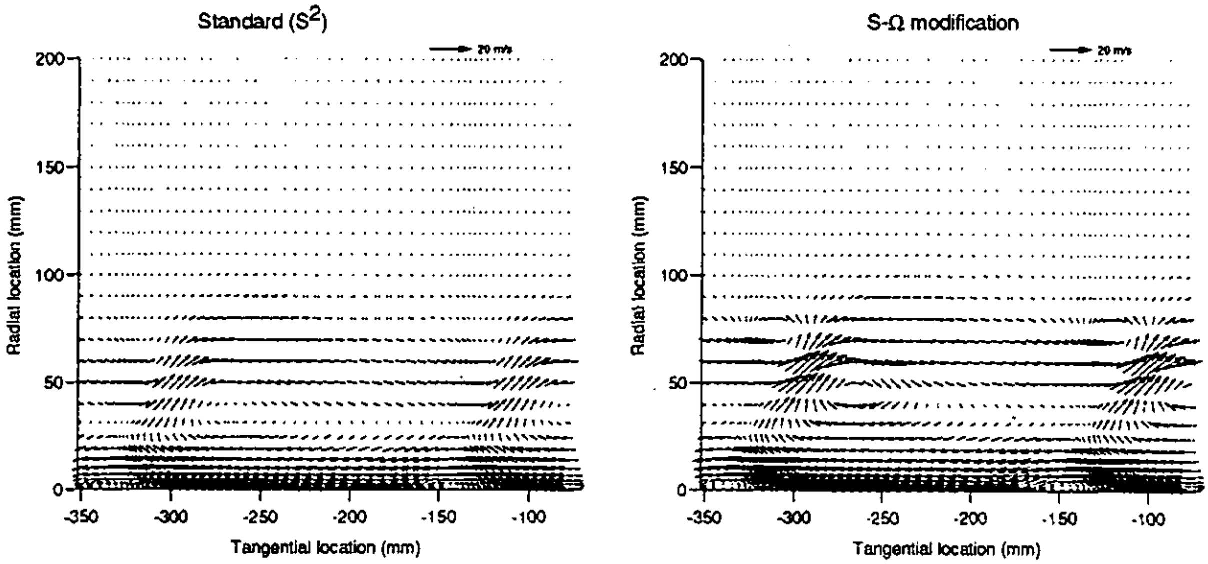

Figure 9: Secondary Flow with k-ε Models

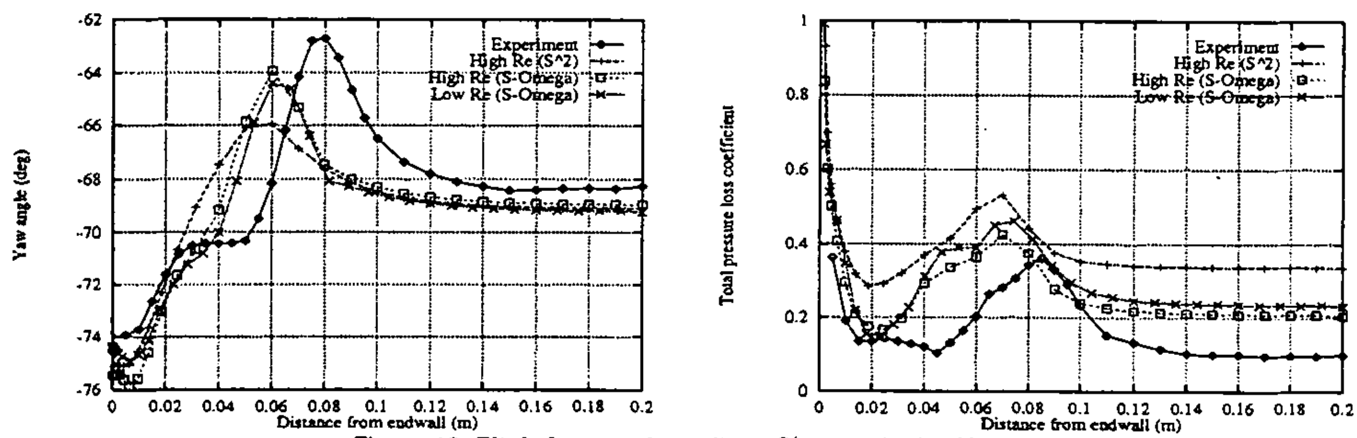

Figure 10: Pitch Averaged results at Slot 10 with k-ε Model

An important requirement for this sort of computational investigation is to have low numerical losses, and in this the pressure correction code proves to be good, as evidenced by the trend that with fully turbulent flow and an excessively low free stream length scale, the 2D loss would fall below the experimental value (Table 3). The importance of the freestream length scale does not seem to have attracted much attention, but these computations show that its specification is very important for the mixing length model used here.

The high Reynolds number k-ε model results have shown (as with previous work, e.g. Gregory-Smith & Cleak, 1992) that generally too much loss and turbulence are generated. This is particularly true when using the quite high measured inlet length scale. The use of the S-Ω modification improved the prediction. The low Reynolds number model which it was hoped would simulate to the transition some extent does not show evidence of doing so. However more work is required in this area, as difficulties with convergence restricted the investigation so far.

CONCLUSIONS

The following conclusions of the study may be drawn:

- The measurement of the intermittency has shown that there are significant regions of laminar flow on the suction surface and end wall, and relaminarisation towards the trailing edge on the pressure surface.
- With a mixing layer model of turbulence, the use of the measured intermittency to specify transition produces excellent computed predictions for both loss and secondary flow field.
- The assumed freestream length scale has a large effect on the results with the mixing length model.

- The high Reynolds number k-ε model of turbulence is also sensitive to high inlet length scale. It gave far too much turbulence and loss at exit. The S-Ω modification improved the predictions significantly.
- The low Reynolds number model did not appear to predict transition at all satisfactorily. However more work is required in this area.
- The pressure correction code gave a degree of grid independency and low numerical loss with a fairly coarse grid (98078 points). It proved to be a good vehicle for this study.

Overall this work shows the importance of transition in the computation of the secondary flows and losses. If the transition is correct, as in the mixing length model specification, the results are very good. However the problem of specifying transition *a priori* remains as a challenge for the future.

ACKNOWLEDGEMENT

The authors gratefully acknowledge support from Rolls-Royce plc. and their permission to publish this paper. The authors are also grateful for additional support from the Engineering and Physical Sciences Research Council.

REFERENCES

Biesinger T.E., (1993) "Secondary Flow Reduction Techniques in Linear Turbine Cascades." PhD. Thesis, University of Durham.

Cleak, J.G.E., Gregory-Smith D.G., Birch N.T., (1991) "Experimental Verification of a 3D Turbulent Flow Calculation in an Axial Turbine Cascade." AGARD CP510, *Techniques for Propulsion Applications*, Paper No. 8.

Cleak J.G.E., Gregory-Smith D.G., (1992). "Turbulence Modelling for Secondary Flow Prediction in a Turbine Cascade." *J. Turbomachinery:* ASME Paper 91-GT-57 Vol.114 No.3, pp.590-598.

Falco R.E., Gendrich C.P. (1990). "The Turbulent Burst Detection Algorithm of Z.Zadric." Near-wall turbulence: 1988 Zoltan Zaric memorial conference, Eds Kline & Afgan, Hemisphere, pp. 911-931

Gregory-Smith D.G., (1993), "The ERCOFTAC Seminar and Workshop on 3D Turbomachinery Flow Predictions, December 1992." ASME Paper No. 93-GT-423

Gregory-Smith D.G., (1995), "Calculations of the Secondary Flow in a Turbine Cascade." International Symposium on Computational Fluid Dynamics in Aeropropulsion, ASME International ME'95 Congress and Exposition, November

Gregory-Smith D.G., Cleak J.G.E., (1992). "Secondary Flow Measurements in a Turbine Cascade with High Inlet Turbulence." *J. Turbomachinery:* ASME Paper No. 90-GT-20, Vol.114 No.1, pp.173-183.

Halstead D.E., Okiishi T.H., Wisler D.C., (1990). "Boundary Layer Transition and Separation on a Turbine Blade in Plane Cascade." AIAA/SAE/ASME/ASEE 26th. Joint Propulsion Conference, Orlando.

Harrison S., (1989). "Secondary Loss Generation in a Linear Cascade of High-Turning Turbine Blades." ASME Paper No. 89-GT-47

Jones W.P. & Launder B.E., (1972). "The Prediction of Laminarization with a Two-Equation Model of Turbulence." Int. J. Heat and Mass Transfer, Vol.15, pp.301-313.

Kato M, & Launder B.E., (1993). "The Modelling of Turbulent Flows around Stationary and Rotating Cylinders." Proc. 9th. Symposium on Turbulent Sheer Flows, Kyoto

Lakshminarayana B., (1991). "An Assessment of Computational Fluid Dynamic Techniques in the Analysis and Design of Turbomachinery." !990 Freeman Scholar Lecture, ASME J. Fluids Engg., Vol.113, pp.315-352.

Launder B.E., & Sharma B.I., (1974). "Application of the Energy Dissipation Model of Turbulence to the Calculation of the Flow near a Spinning Disk." Letters in Heat and Mass Transfer, Vol.1, pp.131-138.

Mayle R.E. (1991). "The Role of Laminar-Turbulent Transition in Gas Turbine Engines." ASME Paper No. 91-GT-261.

Moore H., (1995) "Experiments in a Turbine Cascade for the Validation of Turbulence and Transition Models." PhD. Thesis, University of Durham.

Moore H., Gregory-Smith D.G., (1995) "Turbulence and Transition in Secondary Flows in a Turbine Cascade." AGARD PEP *Loss Mechanisms and Unsteady Flows in Turbomachines*, Derby, May, Paper No. 8

Moore J, Moore J.G., (1985), "Performance Evaluation of Linear Turbine Cascades using Three-Dimensional Viscous Flow Calculations." *J. Turbomachinery*, Vol.109, pp.258-267

Sieverding C.H., (1985), "Recent Progress in the Understanding of Basic Aspects of Secondary Flows In Turbine Blade Passages." ASME, J. Eng. Gas Turbines and Power, Vol.107, pp.248-252.

Walsh J.A., Gregory-Smith D.G. (1987). The Effect of Inlet Skew on the Secondary Flows and Losses in a Turbine Cascade. IMechE C275/87 15-28.

Walker G.J., & Solomon W.J. (1992). "Turbulent Intermittency Measurement on an Axial Compressor Blade." 11th. Australian Fluid Mechanics Conference, University of Tasmania, Hobart, Australia.